Archives of Materials Science and Engineering

Volume 28
Issue 2
February 2007
Pages 105-112

International Scientific Journal
published monthly as the organ of
the Committee of Materials Science
of the Polish Academy of Sciences

The effect of cooling rate on microstructure and mechanical properties of AC AlSi9Cu alloy

L.A. Dobrzański [a],*, R. Maniara [a], J.H. Sokolowski [b]

[a] Division of Materials Processing Technology, Management and Computer Techniques in Materials Science, Institute of Engineering Materials and Biomaterials, Silesian University of Technology, ul. Konarskiego 18a, 44-100 Gliwice, Poland

[b] Light Metals Casting Technology Group 401 Sunset Avenue, Windsor N9B 3P4, Ontario, Canada

* Corresponding author: E-mail address: leszek.dobrzanski@polsl.pl

Received 10.10.2006; accepted in revised form 25.01.2007

ABSTRACT

Purpose: In this work the effect of cooling rate on the size of the grains, SDAS, size of the β precipitation and thermal characteristic results of AC AlSi9Cu cast alloy have been described. The solidification process was studied using the cooling curve and crystallization curve at solidification rate ranging from 0,16 $^{o}Cs^{-1}$ up to 1,04 $^{o}Cs^{-1}$.

Design/methodology/approach: The experimental alloy used in this investigation was prepared by mixing in suitable proportion the AC AlSi5Cu1(Mg) commercial alloys and two master alloys AlSi49 and AlCu55. Thermal analysis tests were made using the UMSA Technology Platform. Cooling curve thermal analysis was performed on all samples using high sensitivity thermocouples of K type that were protected in a stainless steel sheath and data were acquired by a high speed data acquisition system linked to a PC computer. Each chilled sample was sectioned horizontally where the tip of the thermocouple was located and it was prepared by standard grinding and polishing procedures. The final stage of polishing was done using commercial silicon oxide slurry. Optical microscopy was used to characterize the microstructure and intermetallic phases. Secondary dendrite arm spacing measurements were carried out using a Leica Q-Win^{TM} image analyzer. The UTM measurements were carried out using a Zwick testing machine.

Findings: Increasing the cooling rate increases significantly the liquidus temperature, nucleation undercooling temperature, solidification range and decreases the recalescence undercooling temperature. Increasing cooling rate refines all microstructural features including secondary dendrite arm spacing (SDAS) and intermetallic compounds and improves silicon modification level.

Research limitations/implications: The results presented in this paper show results only for the one alloy - AC AlSi9Cu, and for the assessment of the Silicon Modification Level didn't include the arrangement of a Si crystal in a matrix.

Practical implications: The aim of this work is describe in detail the solidification process in a number of AC AlSi9Cu foundry alloy. Cooling rates applied in this experiment occur in cross section of a bloc engine. The results shows the effect of different cooling rates on the microstructural features and the characteristic parameters of the cooling curve of ACAlSi9Cu alloy.

Originality/value: Original value of the work is applied the artificial intelligence for the assessment of the Silicon Modification Level.

Keywords: Aluminum alloys; Cooling rate; Thermal characteristics; Secondary Dendrite Arm Spacing

METHODOLOGY OF RESEARCH, ANALYSIS AND MODELLING

1. Introduction

The increased use of cast aluminum alloys in automotive applications such as engine blocks and cylinder heads creates the need for a deeper understanding of fatigue performance and the influences of processing parameters [1-6]. In designing cast automotive parts, it is important to have an intimate knowledge of how it alloy solidifies at different cross sections of the cast part and how this influences on mechanical properties. This knowledge enables the designer to ensure that the casting will achieve the desired properties for its intended application [9, 10].

Several studies of cast aluminum alloys [11, 12, 13-18] have established that high purity AlSiCu hypoeutectic alloys exhibit three main solidification reactions during the solidification process, starting with the formation of aluminum dendrites (liquidus) followed by the development of two main eutectic phases. The presence of alloying and impurity elements such as: Cu, Mg, Mn, Fe leads to more complex constituents (including intermetallic) that are characterized by metallographic techniques. Bäckerud et al. [12, 15-18] identified the reactions in AC AlSiXCuX, (3XX) alloys and listed four solid state phases, (Table 1).

Table 1.
Reactions occurring during the solidification of the AC AlSiXCuX, (3XX) alloys according to [12, 15-18]

No	Reaction	Temperature [ºC]
1	Development of dendritic network	620-580
2	$L \rightarrow Al+Si+AlFe_5Si$	570-555
3	$L \rightarrow Al+Si+Al_8FeMg_3Si_6+Mg_2Si$	540-500
4	$L \rightarrow Al+Al_2Cu+Si+Al_5Cu_2Mg_8Si_6$	500-470

The reaction occurring during the solidification of the AC AlSiXCuX, (3XX) alloys can be described as fallows [11, 12, 15-18]:

1. A primary α-aluminum network forms between 620-580 ºC. The exact temperature depends mainly on the amount of Si and Cu concentration in the alloy.
2. Within the 570-555 ºC the eutectic mixture of Si and α-aluminum forms, leading to a further localized increase in Cu content of the remaining liquid. The Fe rich phases can also precipitate in this temperature range.
3. At approximately 540 ºC the Mg_2Si and $Al_8Mg_3FeSi_6$ phases begin to precipitate.
4. A reduction in the temperature allows for precipitation of Al_2Cu and $Al_{15}Mg_8Cu_2Si_6$ phases between 500-470 ºC.

A deeper understanding of the solidification processes of the investigated industrial grade alloys requires the addition of grain refiners and eutectic Si modifiers using elements like: Ti, B, Sr, Na, Sb. Grain refiners that affect the morphology of the nucleating grains. Commercial aluminum alloys contain a limited number of active nucleating particles. In addition, these particles have a poor nucleating potency, therefore the melt requires a high degree of undercooling (ΔT_{DN}≈3-5 ºC, Figure 2) before these particles become active. Therefore, the effective melt processing requires the addition of grain refiners like the Al 3%Ti 3%B master alloy. This master alloy contains a large number of insoluble boride particles, which effectively nucleate a great number of aluminum grains. Grain refiners added to the melt produce changes in the following thermal characteristics:

– The nucleation occurs far above the bulk equilibrium temperature T_L, for the liquidus temperature for alloys without grain modifiers (please refer to Figure 2).
– There is no undercooling before the actual growth temperature is reached (the recalescence effect is not present, ΔT_R≈0 ºC, see Figure 2) [5, 17, 18].

Si modifiers (Sr, Na and Sb just to mention the most popular ones) change the morphology of the eutectic silicon crystals from large flakes into fibrous structures resembling a coral like morphology. The growth process of the eutectic silicon crystals is influenced by these additions, and the α+β eutectic reaction temperature is lowered by 5-10ºC [18].

The casting structure developed during solidification is depend not only on the nucleation potential of the melt, but also on the thermal gradient imposed during solidification. Therefore, the casting structural features (grain size, secondary dendrite arm spacing, silicon modification level) can be evaluate by examining the cooling curve parameters [7, 11, 13, 14].

The main aims of the present work are to investigate the effect of different solidification rates on the microstructure features and the characteristic cooling curves parameters of AC AlSi9Cu aluminum alloy.

2. Materials and experimental procedure

The experimental Al–Si–Cu alloy used in this investigation was prepared at the University of Windsor (Canada) in the Light Metals Casting Laboratory, by mixing the AC AlSi5Cu1(Mg) (C 355.2) commercial alloys and two master alloys AlSi49 and AlCu55. The melted test samples were held for 12 hours in Lindberg™ electric resistance furnace at 850±5 ºC under a protective argon gas atmosphere. Before casting the melts were homogenized and degassed with the aim to reduce the hydrogen level below 0.100±0.005 ml H_2/100g of aluminum and the surface was carefully skimmed. A total of 24 samples of the AC AlSi9Cu alloy were prepared and thier chemical compositions was analyzed by Optical Emission Spectroscopy (OES) as per the ASTM E1251 specification. The chemical compositions of this alloys is given in Table 2.

Table 2.
Average chemical composition (wt %) of investigated alloy, equilibrium liquidus temperature - T_L and cooling rate – CR applied in the investigation

Si	Fe	Cu	Mn	Mg	Zn	Ti	T_L, [ºC]	CR, [ºCs^{-1}]
9.09	0.18	1.05	0.38	0.27	9.09	0.09	600	0.16
								0.48
								1.04

Thermal analysis (TA) tests were made using the UMSA Technology Platform [20]. The TA test samples were cast into a 0.25 mm thick stainless steel cap. The mould was isolated at the top and bottom to allow for Newtonian type heat transfer only. A schematic of the experimental set-up for thermal analysis is depicted in Figure 1. In order to obtain statistical confidence, the TA experiments were repeated eight times for each time.

The cooling curve parameters considered in this work schematically depicted in Fig. 2. The aluminum dendritic network nucleation temperature – T_{DN}, the α+β eutectic nucleation temperature – $T_{E(Al+Si)N,}$ the temperature where the new dendritic crystals have grown – T_{Dmin}, the temperature where the new silicon crystals have grown – $T_{E(Al+Si)min}$, were calculated using the first derivative of the cooling curve.

The UMSA test analysis samples were cut longitudinally and then sectioned horizontally approximately 15 mm from the bottom and were prepared for metallographic analysis using standard procedures. Metallographic examinations have been made on Al–Si–Cu cast alloy specimens mounted in thermohardening resins. In order to disclose grain boundaries and the structure and to distinguish precisely the particular precipitaions in Al–Si–Cu alloys as an etching reagent a 0.5–2 % of HBF_4 acid has been used. The observations of the investigated cast materials have been made on the light microscope LEICA MEF4A at magnification 500x, as well as on the electron scanning microscope Opton DSM-940 using a secondary electron detection. For comprehensive characterization of the Si structures a Leica Q-Win™ and a Simagis Research™ Image Analysis System were utilized. The morphology of the sectioned Si particles was characterized by the average area, average perimeter and equivalent diameter while the shape of the Si particles was determined by the aspect ratio and by the circuit factor. The shape and size characterized parameters were used to the Silicon Modification Level (SML) determination. Image Analysis procedures were developed for rapid determination of the parameters, which characterize the size and shape of the Si particles. SML was evaluated by Artificial Neural Network (ANN), which acquired knowledge during the learning process based on the shape and size characterized parameters acquired from the AFS Chart [19].

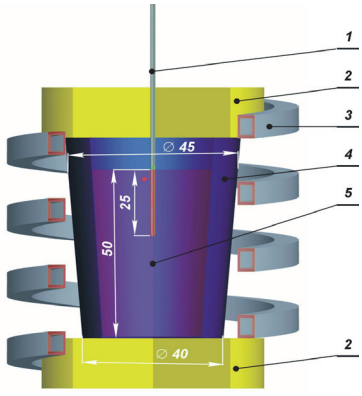

Fig. 1. Schematic of the UMSA Thermal Analysis Platform experimental set-up: 1 – low thermal mass thermocouple, 2 – thermal insulation, 3 – heating and cooling coil, 4 – steel mould, 5 – test sample

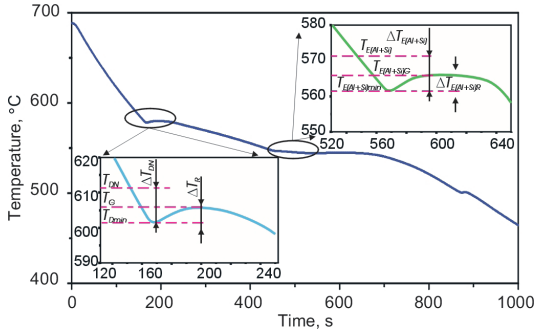

Fig. 2. Generic AC AlSi9Cu alloy cooling curve obtained under the authors non-equilibrium experimental, T_{DN} – aluminum dendritic network nucleation temperature, $T_{E(Al+Si)}$ – equilibrium eutectic temperature, T_{Dmin}, $T_{E(Al+Si)min}$- temperature where the newly nucleated crystal has grown, ΔT_{DN}, $\Delta T_{E(Al+Si)N}$ nucleation undercooling, ΔT_R, $\Delta T_{E(Al+Si)R}$ recalescence temperature

The X-ray qualitative and quantitative microanalysis and the analysis of a surface distribution of cast elements in the examined Al–Si–Cu cast alloy specimens have been made on the Opton DSM-940 scanning microscope with the Oxford EDS LINK ISIS dispersive radiation spectrometer at the accelerating voltage of 15 kV and on the JEOL JCXA 733 x-ray microanalizer. Observations of thin foils structure were carried out in the JEM 3010UHR firmy JEOL transmission electron microscope using an accelerating voltage of 300 kV. Phase composition and crystallographic structure were determined by the X-ray diffraction method using the XPert device with a copper lamp, with 40 kV voltage. The measurement was performed by angle range of 2 Θ: 40º - 110º.

3. Results and discussion

As mentioned before, various researchers have investigated the phases formed during the crystallization process of the Al–Si–Cu alloys. But only several researchers have investigated the influence of solidification rate on phases composition of the AC AlSi9Cu alloy. The analysis of thin foils after the cooling with applied in the experiment solidification rate have validated the fact that the structure of the AC AlSi9Cu cast alloy consists of the solid solution α – Al (matrix) (Fig. 3) and an intermetallic secondary phase β – Si (Fig. 4) in the form large flakes, needle and fibrous precipitations, depending on the applied cooling rate. Moreover, the examinations of the thin aluminum cast alloy foils confirm the existence of an intermetallic phases: Al_2Cu and $AlFe_5Si$. The chemical composition examinations with the use of the EDS dispersive radiation spectrometer as well as literature data, confirm, that in investigated alloy occurring $Al_8FeMg_3Si_6$ phase. This phase forms with α–Al, β–Si and Al_2Cu multicomponent eutectic.

According to the X–ray phase analysis, the investigated AC AlSi9Cu alloy cooled wit solidification rate: 0,16, 0.48 and 1.04 ºC s^{-1} is composed of two phases (Fig. 5): α–Al solid solution as matrix and β–Si as a component of α+β eutectic or Si primary precipitation. In the diffraction pattern of the matrix, the {200}

Al–diffraction line has very intensity. The diffraction lines of the Si–phases don't reveal such a intensity. Based on the X–ray phase analysis was found, that change of solidification rate don't influence on the phases composition of investigated alloy. The X–ray phase analysis don't ravel occurring of Al_2Cu, $AlFe_5Si$ and $Al_8FeMg_3Si_6$ phases, what suggested that the fraction volume of these phases is below 3%.

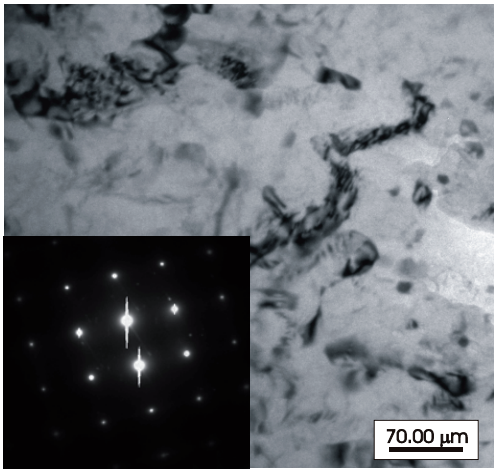

Fig. 3. TEM image of the AC AlSi9Cu alloy cooled with solidification rate 0,16 ºCs^{-1} with selected area diffraction pattern

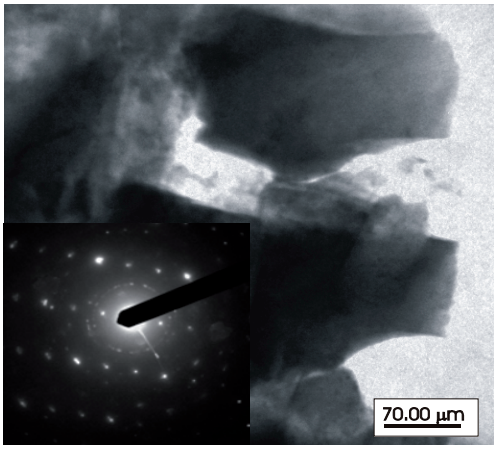

Fig. 4. TEM image of the AC AlSi9Cu alloy cooled with solidification rate 0,48 ºCs^{-1} with selected area diffraction pattern

Result of the surface decomposition of elements and the x-ray, quantitative micro analysis made using the EDS energy dispersive radiation spectrometer, the presence of the main alloy additions Al, Si, Cu and also Fe and Mg included in the aluminum cast alloys in as-cast state cooled with different cooling rate (Fig. 6).

The cooling curves recorded for AC AlSi9Cu alloy at various cooling rates are shown in Fig. 7. It is seen that formation temperatures of the various phases are changed when the cooling rate is increased. The shift magnitude increases with an increasing cooling rate. This shift changes the characteristic parameters of thermal analysis particularly in the liquidus region.

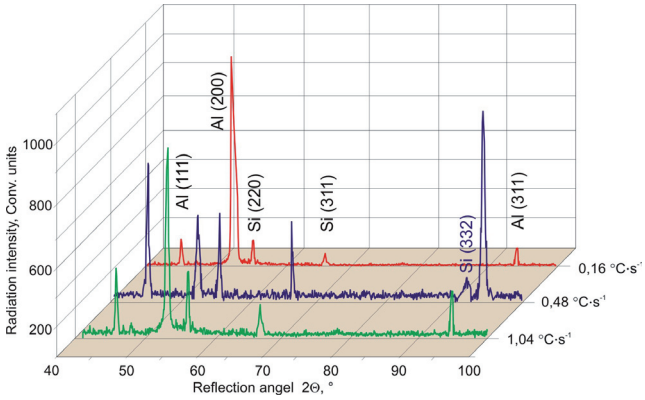

Fig. 5. XRD patterns of the AC AlSi9Cu casting alloy at various solidification conditions

The cooling rate is proportional to the heat extraction from the sample during solidification. Therefore, at a low cooling rate (0.16 ºC·s^{-1}), the rate of heat extraction from the sample is slow and the slope of the cooling curve is small. So, it creates a wide cooling curve. But, at a high cooling rate (1.04 ºC·s^{-1}) the rate of heat extraction from the sample is fast, the slope of the cooling curve is steep and it makes a narrow cooling curve.

Figure 8 shows the variation of the aluminum nucleation temperature as a function of cooling rate and the variation of the Al nucleation undercooling and recalescence temperature. It is evidence from the plot, that the Al nucleation temperature increase with increase cooling rate from 0.16 to 1.04 ºC·s^{-1}, the Al nucleation temperature increases from 586.55 to 605.75°C. Increasing the cooling rate increases the heat extraction. Therefore, the melt is cooled to a lower temperature than the equilibrium melting point. Due to the increase the cooling rate the nucleation undercooling increase. The phenomena of an increase in the nucleation temperature with an increase in the solidification rate depends on the mobility of the clusters of atoms in the melt. These groups of the froze atoms produces the fluctuation clusters and fluctuation embryos, which are the nucleation primers. The increase of the cooling rate with an increase amount of the nucleation primers and reduction of the recalescence temperature is well established fact. This effect have influence on the grain size. Figure 9 shows the variation of the grain size and secondary dendrite arm spacing as a function of cooling rate. As seen on the picture the increase cooling rate decrease strongly the grain size and SDAS.

Three micrographs from samples AC AlSi9Cu alloy cooled with cooling rate: 0.16, 0.48 and 1.04 ºC s^{-1} are shown in Fig. 10.

The microstructures of the alloy include α–Al dendrites, β–eutectic silicon and intermetallic phases such as Al_5FeSi, Mg_2Si, $Al_5Cu_2Mg_8Si_6$ and Al_2Cu (Cu rich phase).

The reduction of (SDAS) is clearly evident from this pictures. The variation of SADAS has been showed graphically in Fig. 9. SDAS is stricte depending on the cooling rate. In the highest cooling rate, the SDAS is fine (≈26.6 µm) and easily visible. For the sample that was cooled with lowest cooling rate, the SDAS is large (≈79.06 µm). Therefore the alloy's design and process engineers have a wide range of solidification rates (process parameters) to chose from.

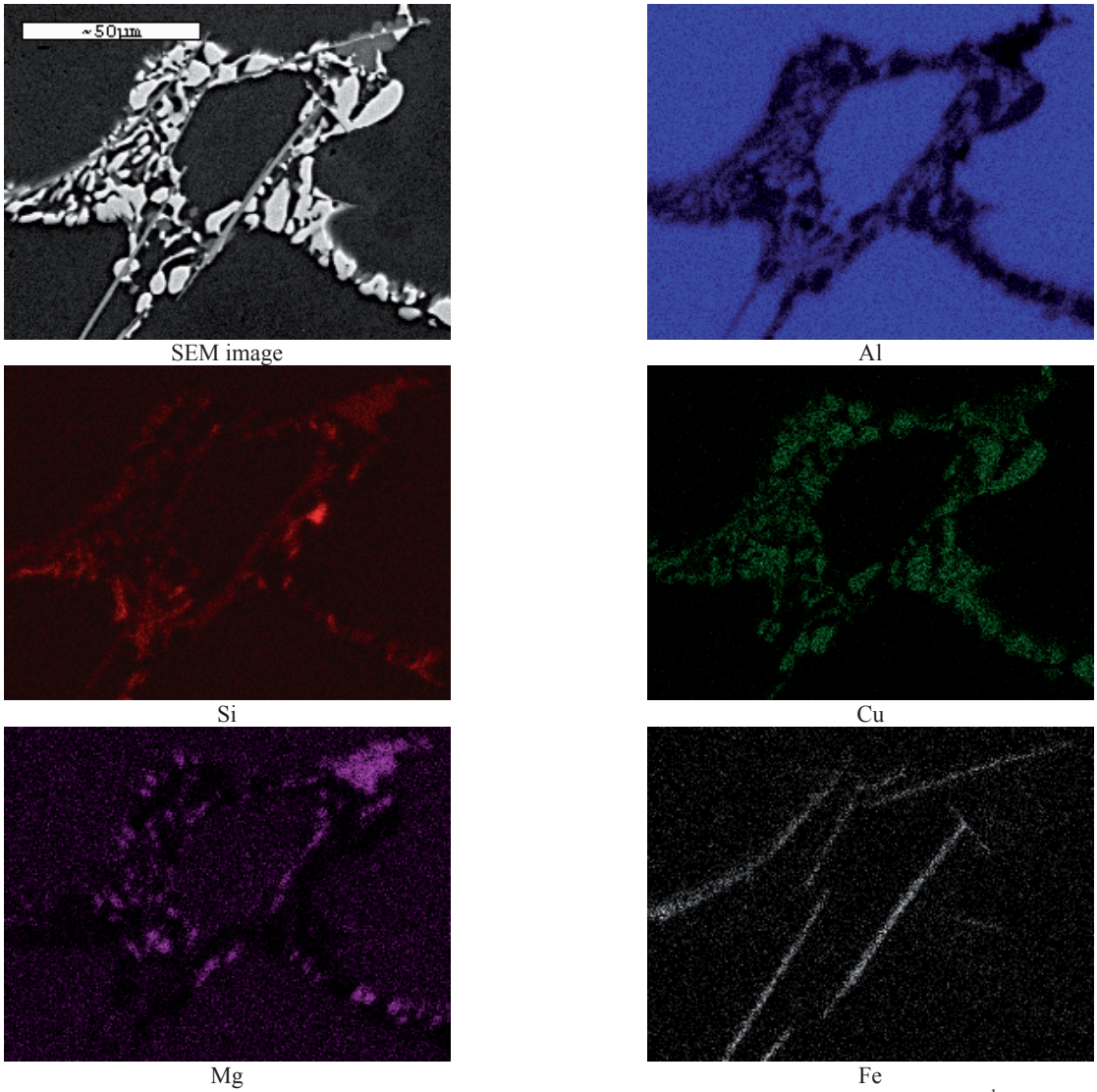

Fig. 6. The area analysis of chemical elements alloy AC AlSi9Cu after cooling witch 0.16 ºCs^{-1}

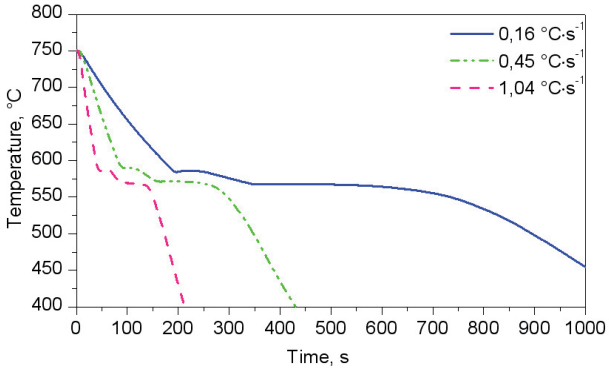

Fig. 7. Cooling curves of AC AlSi9Cu alloy at various solidification conditions

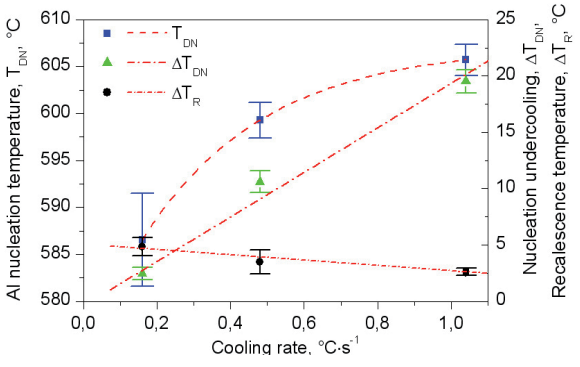

Fig. 8. Variation of the Al nucleate temperature as a function of cooling rate and variation of the Al nucleate undercooling and recalescence temperature as a function of cooling rate

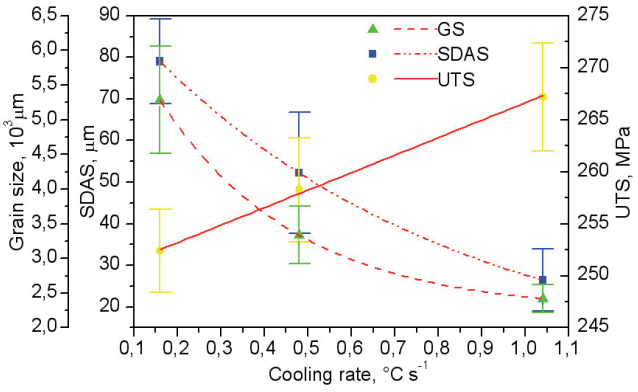

Fig. 9. Variation of the grain size SDAS and UTS as a function of cooling rate

Mechanical properties of the aluminum alloys are strongly dependent on the effect of SDAS. Tensile properties increase with a decrease the SDAS. Investigations results shows, the increase the cooling rate from 0.16 ºC·s^{-1} to 1.04 ºC·s^{-1} influence on the reduction of the SDAS, what have influence on the ultimate tensile strength (UTS). The UTS increase from 252 MPa for lowest cooling rate to 267 MPa for highest cooling rate (Fig. 9).

The eutectic compositions of the binary Al+Si alloy is close to 12% Si below this concentration aluminum precipitate form from the liquid as the primary phases in the form of dendrites, above this concentration primary silicon particles form from the liquid upon cooling. The size of silicon particles in Al-Si alloys are depend of the solidification range and chemical composition and if is change the cooling rate can by controlled by the same way like the size of the grains.

Figure 11 shows the variation of the α+β eutectic nucleation temperature. As the cooling rate increase from 0.16 to 1.04 ºC·s^{-1}, the α+β eutectic nucleation temperature increases from 559 to 562 °C. Increase of cooling rate affected to a increase of α+β eutectic nucleation undercooling and decrease of recalescence temperature. The variation of α+β eutectic nucleation undercooling and recalescence temperature shows Fig. 12. In comparison of microstructure shows on Fig. 10 it can be, that with increase of cooling rate the eutectic intermetallic distance decreases.

In the investigated alloy, the increase solidification rate results in a significant reduction of size of the Si particles (from ≈57 µm^2 for the lowest solidification rate to ≈22 µm^2 for the highest solidification rate). Figure 13 shows the effect of the solidification rate on the percent of Silicon Modifications Level (SML) of the α+β eutectic.

The general trend indicates that an increased solidification rate significantly increases that percent of SML. The tested solidification rates very significantly change the morphology of the eutectic silicon crystals from large flakes – SML1 into a fibrous structure–SML 2, a fibrous structure resembling a coral type of the structure–SML 3, to fain-grained structure–SML 4, SML5.

The solidification range is defined as the difference in temperature between the Al nucleation temperature and the solidus temperature. The thermal modification of the grains SDAS and α+β eutectic has influence on the improve the alloy quality.

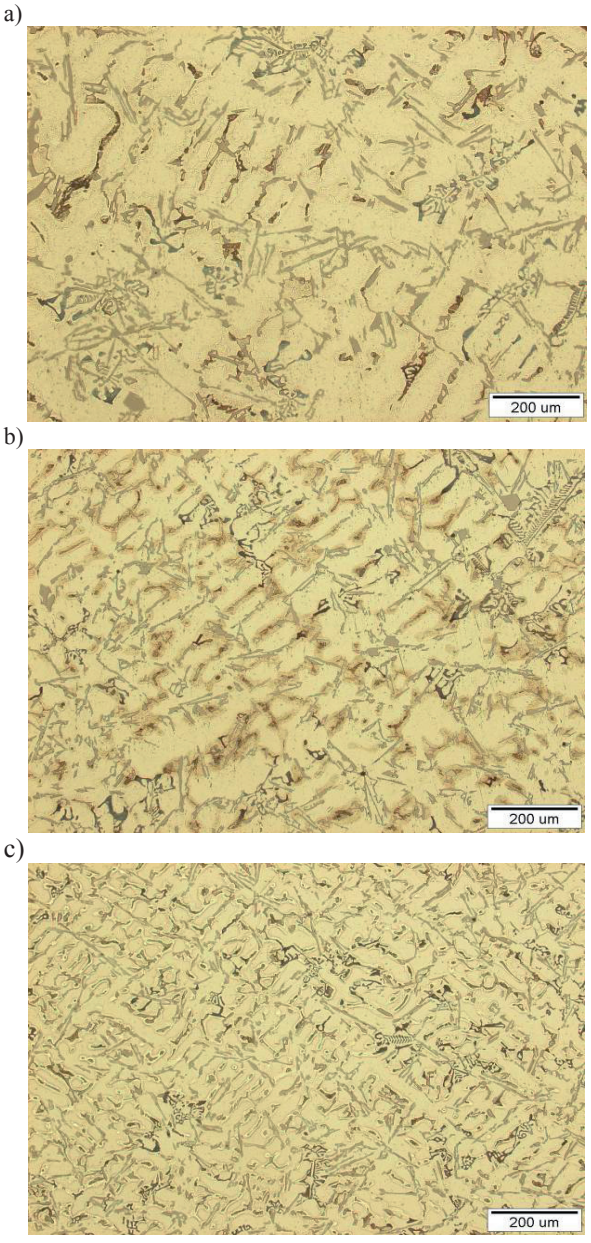

Fig. 10. Micrographs revealing the microstructures of AC AlSi9Cu that solidified: a) 0.16 ºC s^{-1};b) 0.48 ºC s^{-1}, c) 1.04 ºC s^{-1}

Very imported input parameters for any solidification modeling system are solidification range and solidification time. Total solidification time is also the time interval between the start and end of solidification. Figure 14 shows the effect of cooling rate on the solidification range (T_{SR}) and solidification time (t_{SR}). As the cooling rate increases from 0.16 °C/s to 1.04 °C the solidification range increase about 40 °C, but total solidification time decrease about 617 s (about 10 minutes). It can also be seen in Fig. 7 that a cooling curve obtained at the higher cooling rate has a shorter solidification time and larger solidification range.

Solidification times is related to the cooling rate according to the equation proposed by Kumar'a [7, 14].

$$t_{SR} = A(CR)^{-n} \quad (1)$$

where A and n are constants of the equation.

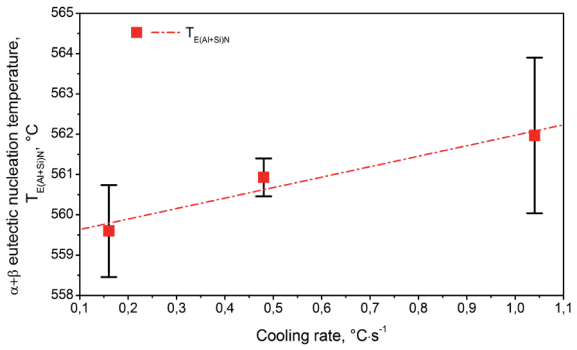

Fig. 11. Variation of the α+β eutectic nucleate temperature as a function of cooling rate

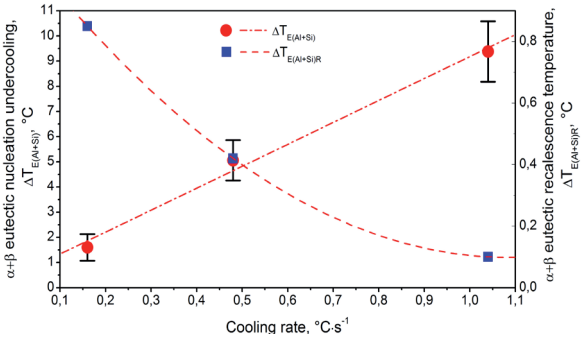

Fig. 12. Variation of the α+β eutectic nucleation undercooling and recalescence temperature as a function of cooling rate

4. Conclusions

The effect of the cooling rate on the structural features such as SDAS, grain size, eutectic silicon, intermetallic phases and thermal analysis characteristic parameters were examined. The results are summarized as follows:

1. Solidification parameters are affected by the cooling rate. The formation temperatures of various phases are changed with an increasing cooling rate.
2. Increasing the cooling rate increases significantly the Al nucleate temperature, nucleation undercooling temperature, solidification range and decreases the recalescence undercooling temperature. These phenomena lead to an increased number of nucleus that affect the size of the grains and the Secondary Dendrite Arm Spacing (SDAS).
3. As expected, the SDAS decreases with increasing cooling rate and the observed variation of the SDAS with cooling rate is in excellent agreement with the predictions of the microsegregation model. The predictions did not involve the adjustment of a fitting parameter.
4. An increase of the cooling rate provided to refine the size of the secondary phase intermetallics and also alter their morphology towards equiaxed by reducing the aspect ratio. This is attributed to the process of repeated nucleation of the intermetallic phases during eutectic solidification.

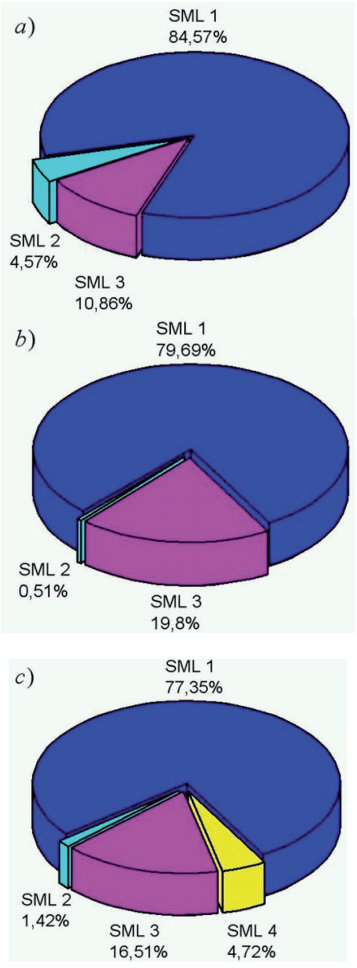

Fig. 13. Effect of the solidification rate on the percent of Silicon Modifications Level (SML) of the α+β eutectic

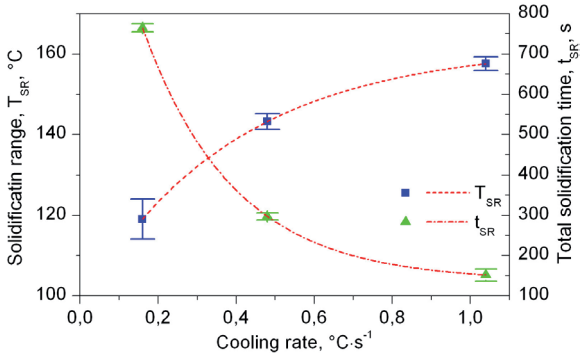

Fig. 14. Effect of the cooling rate on the solidification range and total solidification time

Additional information

The presentation connected with the subject matter of the paper was presented by the authors during the 14th International Scientific Conference on Achievements in Mechanical and Materials Engineering AMME'2006 in Gliwice-Wisła, Poland on 4th-8th June 2006.

References

[1] G. Mrówka–Nowotnik, J. Sieniawski, M. Wierzbińska, Analysis of intermetalic particles In AlSi1MgMn aluminum alloy, Journal of Achievements in Materials and Manufacturing Engineering 20 (2007) 155-158.

[2] L.A. Dobrzański, R. Maniara, J.H. Sokolowski, The effect of cast Al-Si-Cu alloy solidification rate on alloy thermal characteristic, Journal of Achievements in Materials and Manufacturing Engineering 17 (2006) 217-220.

[3] M. Wierzbińska, J. Sieniawski, Effect of morphology of eutectic silicon crystals on mechanical properties and cleavage fracture toughness of AlSi5Cu1 alloy, Journal of Achievements in Materials and Manufacturing Engineering 14 (2006) 31-36.

[4] M. Kciuk, Structure, mechanical properties and corrosion resistance of AlMg5 alloy, Journal of Achievements in Materials and Manufacturing Engineering 17 (2006) 185-188.

[5] L.Y. Pio, S. Sulaimin, A.M. Hamouda, Grain refinement of LM6Al–Si alloy sand castings to enhance mechanical properties, Journal of Materials Processing Technology 162-163 (2005) 435-441.

[6] J.G. Kauffman, E. L. Rooy, Aluminum Alloy Castings, ASM International, Ohio 2005.

[7] S.G. Shabestari, M. Malekan, Thermal Analysis Study of the Effect of the Cooling Rate on the Microstructure and solidification parameters of 319 aluminum alloy, Canadian Metallurgical Quarterly 44 (2005) 305-312.

[8] L.A Dobrzański, K. Labisz, R. Maniara, Microstructure investigation and hardness measurement in Al-Ti alloy with additions of Mg after heat treatment, Proceedings of the 13th International Scientific Conference on Achievements in Mechanical and Materials Engineering AMME'2005, Gliwice-Wisła, 2005, 147-150.

[9] Z. Li, A.M. Samuel, F.H. Samuel, C. Ravindran, S. Valtierra, H.W. Doty, Parameters controlling the performance of AA319-type alloys Part I. Tensile properties, Materials Science and Engineering 367 (2004) 96-110.

[10] S.G. Shabestari, H. Moemeni, Effect of copper and solidification conditions on the microstructure and mechanical properties of Al–Si–Mg alloys, Journal of Materials Processing Technology 153-154 (2004) 193-198.

[11] R. MacKay, M. Djurdjevic, J.H. Sokolowski, The effect of cooling rate on the fraction solid of the metallurgical reaction in the 319 alloy, AFS Transaction, 2000.

[12] C.H. Cáceres, M.B. Djurdjevic, T.J. Stockwell, J.H. Sokolowski, Cast Al: The effect of cu content on the level of microporosity in Al-Si-Cu-Mg casting alloys, Scripta Materiala, 1999.

[13] J.M. Boileau, J.W. Zindel, J.E. Allison, The Effect of Solidification time on the mechanical properties in a cast A356-T6 aluminum alloy, Society of Automotive Engineers, Inc, 1997.

[14] P. Kumar, J.L. Gaindhar, DAS, Solidification time and mechanical properties of Al-11%Si alloys V-processed castings, AFS Transactions, 105, 1997.

[15] A.M. Samuel, A. Gotmare, F.H. Samuel, Effect of solidification rate and metal feedability on porosity and SiC/Al_2O_3 particle distributing in an Al-Si-Mg (359) alloy, Composite Science and Technology, 1994.

[16] L. Bäckerud, E. Król, J. Tamminen: Solidification characteristics of aluminum alloys, Vol. 1, Universitetsforlaget, Oslo, 1986.

[17] L. Bäckerud, G. Chai, J. Tamminen, Solidification characteristics of aluminum alloys, AFS, vol. 2, 1992.

[18] L. Bäckerud, G. Chai, Solidification Characteristics of aluminum alloys, Vol. 3, AFS, 1992.

[19] American Foundry Society, (AFS), Chart for microstructure control in hypoeutectic aluminum silicon alloys, American Foundry Society, Inc., Des Plaines, Illinois, 1990.

[20] http://www.uwindsor.ca/umsa.